P2.5 SURFACE EMISSIVITY MAPS FOR SATELLITE RETRIEVAL OF THE LONGWAVE RADIATION BUDGET

Shashi K. Gupta and Anne C. Wilber
Analytical Services and Materials, Inc., Hampton, Virginia

David P. Kratz
NASA Langley Research Center, Hampton, Virginia

1. INTRODUCTION

Accurate accounting of surface emissivity is essential for retrievals of surface temperature from remote sensing measurements (Wan and Dozier 1996) and for the calculation of the longwave (LW) surface radiation budget (SRB). Retrieving the LW SRB is an important objective of NASA's Clouds and the Earth's Radiant Energy System (CERES) project (Wielicki et al. 1996). Most studies in the past, dealing with such retrievals, assumed that the emissivity for all surface types and across the LW spectrum was equal to unity. There is strong evidence, however, to show that the emissivity of many surfaces is significantly lower than unity, and that the emissivity varies considerably across the LW spectrum.

There has been some effort accompanied with limited success in relating infrared emissivity of vegetated surfaces with the Normalized Difference Vegetation Index (NDVI) derived from the Advanced Very High Resolution Radiometer (AVHRR; e.g., Olioso 1995). In the future, satellite instruments like the Advanced Spaceborne Thermal Emission and Reflection Radiometer (ASTER) and the Moderate-Resolution Imaging Spectroradiometer (MODIS) will retrieve surface emissivity using temperature-emissivity separation algorithms. Presently, however, there is little information available on surface emissivity variability to meet the needs of a project like CERES which has been flying on the Tropical Rainfall Measuring Mission (TRMM) satellite since late 1997.

We have developed global maps of surface emissivity for the broadband LW region, the thermal infrared window region (8-12 μm), and 12 narrow spectral bands used in the LW portion of the Fu-Liou radiative transfer code (Fu and Liou 1992). The primary purpose of developing these maps was to improve the retrievals of surface, atmospheric, and top-of-atmosphere (TOA) radiation budgets from the current CERES measurements.

Corresponding author address: Shashi K. Gupta, Analytical Services and Materials, Inc., 1 Enterprise Parkway, Suite 300, Hampton, VA 23666;
e-mail, s.k.gupta@larc.nasa.gov

2. LABORATORY DATA

Salisbury and D'Aria (1992) made extensive measurements of the spectral reflectances of surface materials in the 2-16 μm region, and made the measurements available to the scientific community as the Johns Hopkins Spectral Library. The ASTER team is using this library and created an easily accessible database which is located at the website:

http://asterweb.jpl.nasa.gov/speclib/.

We chose and obtained spectral reflectance data for 10 different surface materials from the above site and used them for deriving the emissivities. The chosen surface materials were: grass, conifer, deciduous, fine snow, medium snow, coarse snow, frost, ice, sea water, and quartz sand.

3. METHODOLOGY

The spectral reflectances of surface materials were converted to corresponding spectral emissivities using the energy conservation principle and Kirchhoff's law. From energy conservation considerations

$$A_\lambda + R_\lambda + T_\lambda = 1 \quad (1)$$

where A_λ, R_λ, and T_λ are absorptance, reflectance, and transmittance respectively. The transmittance of the surfaces was assumed to be zero. Applying Kirchhoff's law which states that under conditions of thermodynamic equilibrium, the absorptance and emittance are equal, we obtain

$$\varepsilon_\lambda = 1 - R_\lambda. \quad (2)$$

Spectral emissivity of the conifer surface in the 4-16 μm region computed from the reflectance database using Eq. (2) is shown in Fig. 1. Dashed vertical lines in Fig. 1 show wavelength ranges for nine of the 12 LW bands of the Fu-Liou code. The next two bands cover the wavelength range up to 35.7 μm, and the last band covers the entire infrared spectrum beyond 35.7 μm. The Fu-Liou code is being used by the Surface and Atmospheric Radiation Budget (SARB) working group of CERES for computing radiation budgets of the atmospheric column and the surface.

Average emissivities over each of the 12 LW bands for the 10 surface materials were computed by averaging the high resolution values like those shown in Fig. 1 for the conifer surface. Since measured values were available only up to 16 μm, the value at 16 μm was adopted for all wavelengths beyond 16 μm. A broadband LW emissivity for each surface material was then computed by averaging the 12 band values weighted with the Planck function energy distribution. A similar procedure was applied for computing average emissivities of all surface materials for the 8-12 μm window. The window was divided into three narrow bands in order to account for the large variation of spectral emissivity across the 8-12 μm region.

Emissivity maps were developed by implementing the following steps. The 10' lon. x 10' lat. global scene type map used by the SARB working group was used to classify the surface into 18 scene types. The scene types for this map were adopted from the International Geosphere Biosphere Programme (IGBP) classification for the Earth's surface with an additional scene type for tundra. The 10 surface materials were then associated, individually or in combination, with each of the surface types, based on the best judgment of the authors. The 18 surface types and their associations with the surface materials are shown in Table 1. An emissivity value was assigned to each grid box based on its association with the surface materials. The same procedure was followed for developing maps for the broadband LW, the 8-12 μm window, and the 12 Fu-Liou bands.

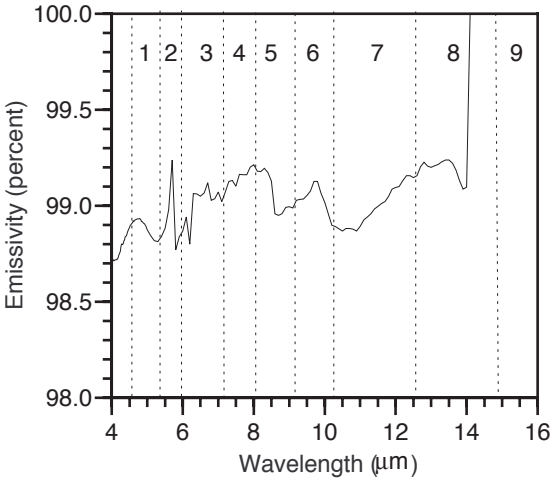

Figure 1. Locations of Fu-Liou Bands Relative to Laboratory Measurements of Conifer Sample

Table 1. Assignment of laboratory measurements to surface types.

Type ID	IGBP type	Spectral library
1	Evergreen Needleleaf Forest	Conifer
2	Evergreen Broadleaf Forest	Conifer
3	Deciduous Needleleaf Forest	Deciduous
4	Deciduous Broadleaf Forest	Deciduous
5	Mixed Forest	1/2 Conifer + 1/2 Deciduous
6	Closed Shrublands	1/4 Quartz sand + 3/8 Conifer + 3/8 Deciduous
7	Open Shrubland	3/4 Quartz sand + 1/8 Conifer + 1/8 Deciduous
8	Woody Savannas	Grass
9	Savannas	Grass
10	Grasslands	Grass
11	Permanent Wetlands	1/2 Grass + 1/2 Seawater
12	Croplands	Grass
13	Urban	Black Body
14	Cropland/Mosaic	1/2 Grass + 1/4 Conifer + 1/4 Deciduous
15	Snow and Ice	Mean Of Fine, Medium, and Coarse snow and Ice
16	Barren	Quartz sand
17	Water Bodies	Seawater
18	Tundra	Frost

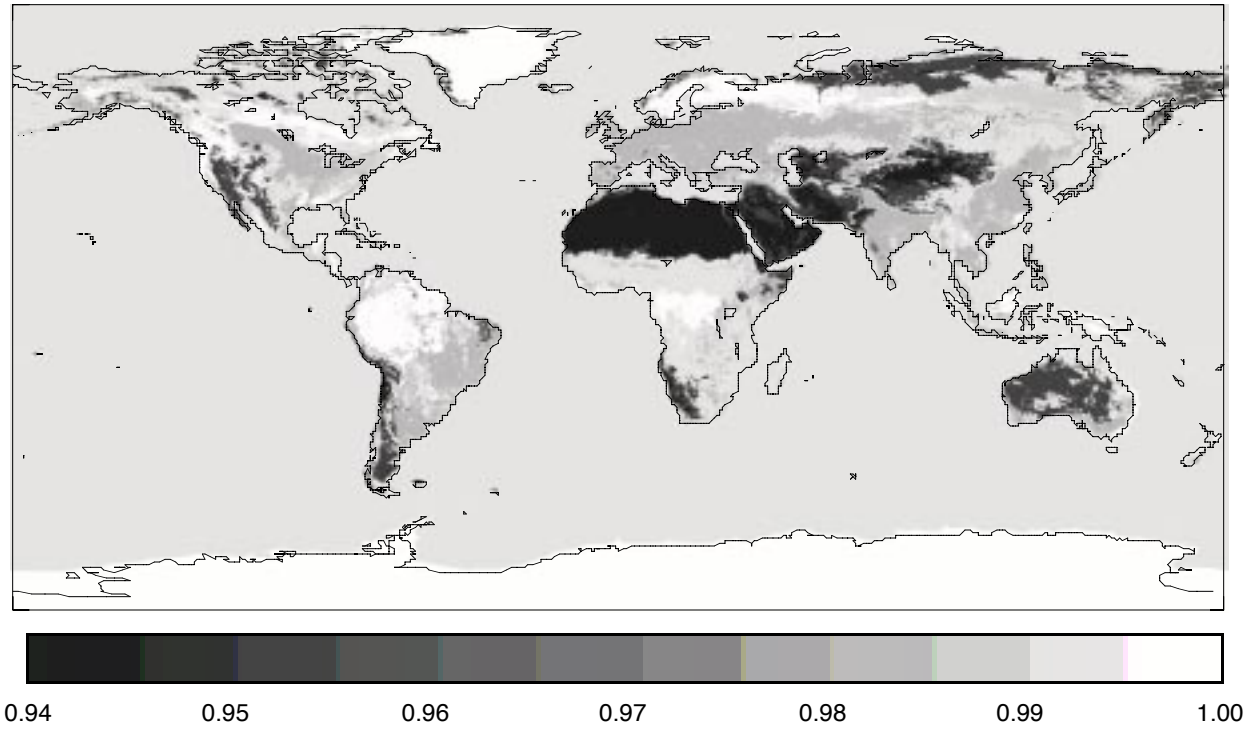

Figure 2. Broadband surface emissivity.

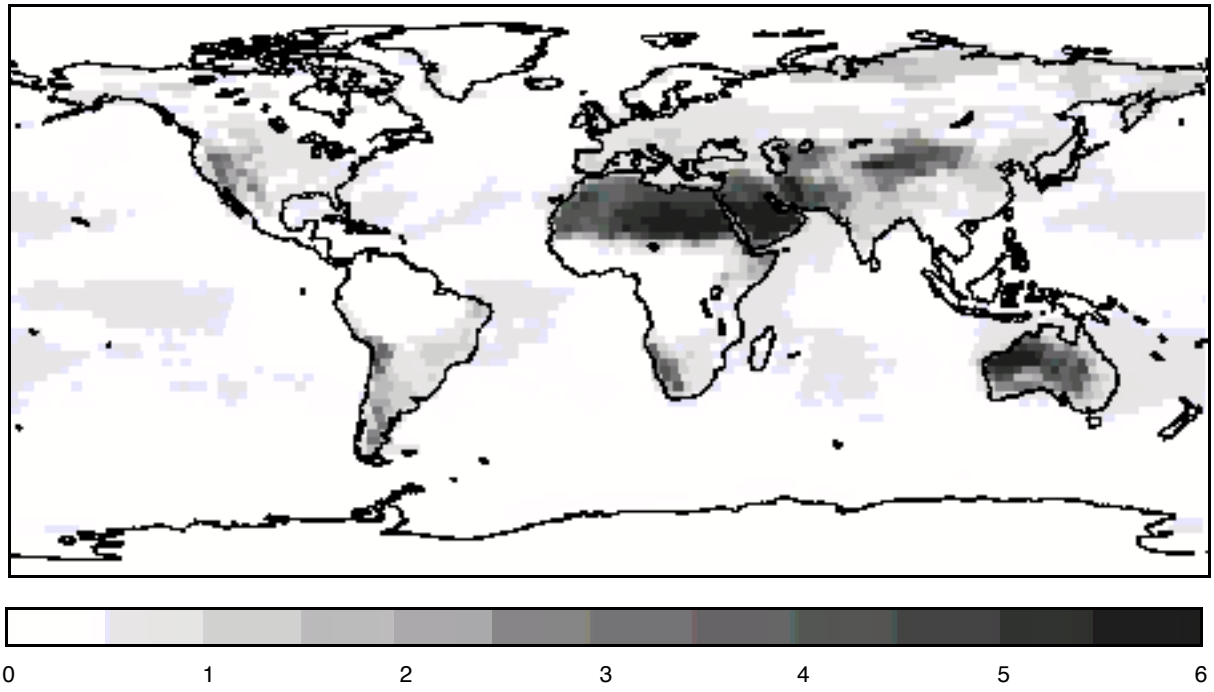

Figure 3. Difference in Surface Net Longwave Flux (W m^{-2})

4. RESULTS

Figure 2 shows the global map of the broadband LW surface emissivity derived here at the 10' lon. x 10' lat. resolution. Values range from 0.94 over desert areas to 1.00 over snow/ice covered regions of the globe, and 0.99 over most of the oceans. Similar maps (not shown here) were developed for the 8-12 μm window, and for each of the 12 Fu-Liou bands. Emissivities over desert regions were considerably lower in the 8-12 μm window (0.87) than for the broadband. Our broadband emissivity map was used in conjunction with a LW surface radiation model (Gupta et al. 1992) to assess the effect on the net LW flux field at the surface. Differences between the net LW fluxes computed with this map and those with an emissivity of unity are presented in Fig. 3. The figure shows that differences are as large as 6 Wm^{-2} over desert areas and upto 3 Wm^{-2} over large parts of land areas.

5. CONCLUDING REMARKS

This paper presents a brief description of the procedure used to produce global surface emissivity maps for the broadband LW, the 8-12 μm window, and 12 narrow LW bands. For a detailed description of the methodology and the input data, the reader is referred to Wilber et al. (1999). These maps are based on a time-independent surface type map published by the IGBP, and laboratory measurements of spectral reflectances of surface materials. These maps represent a first attempt to characterize emissivity based on surface types, and many improvements to the methodology presented here are already underway. Effects of viewing zenith angle and sea state on the emissivity of ocean surface (Smith et al. 1996, Wu and Smith 1997, Masuda et al. 1988) will be taken into account. Measurements form ASTER and MODIS will be incorporated as they become available. Seasonal variation of emissivity based on changes in the characteristics of vegetation will be considered, and the variability of emissivity of barren land areas will be accounted for with the use of Zobler World Soil Maps (Zobler 1986). The current maps have been made available to the scientific community from the web site:

http://tanalo.larc.nasa.gov:8080/surf_htmls/SARB_surf.html

6. REFERENCES

Fu, Q. and K. N. Liou, 1992: On the correlated k-distribution method for radiative transfer in nonhomogeneous atmospheres. J. Atmos. Sci., **49**, 2139–2156.

Gupta, S. K., W. L. Darnell, and A. C. Wilber, 1992: A parameterization for longwave surface radiation from satellite data: Recent improvements. J. Appl. Meteor., **31**, 1361–1367.

Masusda, K., T. Takashima, and Y. Takayama , 1988: Emissivity of pure and sea waters for the model sea surface in the infrared window regions. Remote Sens. Environ., **24**, 313–329.

Olioso, A., 1995: Simulating the relationship between thermal emissivity and Normalized Difference Vegetation Index. Int. J. Remote Sens., **16**, 3211–3216.

Salisbury, J. W. and D. M. D'Aria, 1992: Emissivity of terrestrial materials in the 8–14 mm atmospheric window. Remote Sens. Environ., **42**, 83–106.

Smith, W. L., R. O. Knuteson, H. E. Revercomb, W. Feltz, H. B. Howell, W. P. Menzel, N. R. Nalli, O. Brown, J. Brown, P. Minnett, and W. McKeown, 1996: Observations of the infrared radiative properties of the ocean- Implications for the measurement of sea surface temperature via satellite remote sensing. Bull. Amer. Meteor. Soc. **77**, 41–51.

Wan, Z. and J. Dozier, 1996: A generalized split-window algorithm for retrieving land-surface temperature from space. IEEE Trans. Geosci. Remote Sens., **34**, 892–905.

Wielicki, B. A., B. R. Barkstrom, E. F. Harrison, R. B. Lee III, G. L. Smith, and J. E. Cooper, 1996: Clouds and the Earth's Radiant Energy System (CERES): An Earth Observing System experiment. Bull. Amer. Meteor. Soc., **77**, 853–868.

Wilber, A. C., D. P. Kratz, and S. K. Gupta, 1999: Surface emissivity maps for use in retrievals of longwave radiation. NASA Technical Paper (to be published).

Wu, X. and W. L. Smith, 1997: Emissivity of rough sea surface for 8–13 mm: Modeling and verification. Appl. Opt., **36**, 2609–2619.

Zobler, L., 1986: A world soil file for global climate modeling. NASA TM 87802, 35 pp.